

This article is published as part of the *Dalton Transactions* themed issue entitled:

New Talent Asia

*Highlighting the excellent work being carried out by younger members
of the inorganic academic community in Asia*

Guest Editor Masahiro Yamashita
Tohoku University, Japan

Published in [issue 10, 2011](#) of *Dalton Transactions*



Image reproduced with permission of Kenneth Kam-Wing Lo

Articles in the issue include:

PERSPECTIVES:

[Pyrazolin-4-ylidenes: a new class of intriguing ligands](#)

Yuan Han and Han Vinh Huynh, *Dalton Trans.*, 2011, DOI: 10.1039/C0DT01037E

[Solvent induced molecular magnetic changes observed in single-crystal-to-single-crystal transformation](#)

Zheng-Ming Hao and Xian-Ming Zhang, *Dalton Trans.*, 2011, DOI: 10.1039/C0DT00979B,

ARTICLES:

[Negative thermal expansion emerging upon structural phase transition in \$ZrV_2O_7\$ and \$HfV_2O_7\$](#)

Yasuhisa Yamamura, Aruto Horikoshi, Syuma Yasuzuka, Hideki Saitoh and Kazuya Saito
Dalton Trans., 2011, DOI: 10.1039/C0DT01087A

[Preparation of surface molecularly imprinted Ru-complex catalysts for asymmetric transfer hydrogenation in water media](#)

Zhihuan Weng, Satoshi Muratsugu, Nozomu Ishiguro, Shin-ichi Ohkoshi and Mizuki Tada
Dalton Trans., 2011, DOI: 10.1039/C0DT00950D

Visit the *Dalton Transactions* website for more cutting-edge inorganic and organometallic research
www.rsc.org/dalton

Heteroleptic ruthenium complexes containing uncommon 5,5'-disubstituted-2,2'-bipyridine chromophores for dye-sensitized solar cells†

Feng-Rong Dai,^a Wen-Jun Wu,^b Qi-Wei Wang,^a He Tian^{*b} and Wai-Yeung Wong^{*a}

Received 18th August 2010, Accepted 28th September 2010

DOI: 10.1039/c0dt01043j

Four new heteroleptic ruthenium sensitizers [Ru(4,4'-carboxylic acid-2,2'-bipyridine)(L)(NCS)₂] (L = 5,5'-bis(4-octylthiophen-2-yl)-2,2'-bipyridine (**1**), 5,5'-bis(*N,N*-diphenyl-4-aminophenyl)-2,2'-bipyridine (**2**), 5,5'-bis(5-(*N,N*-diphenyl-4-aminophenyl)-thiophen-2-yl)-2,2'-bipyridine (**3**) and 5,5'-bis(4-octyl-5-(*N,N*-diphenyl-4-aminophenyl)-thiophen-2-yl)-2,2'-bipyridine (**4**)) were synthesized, characterized by physicochemical and computational methods, and utilized as photosensitizers in nanocrystalline dye-sensitized solar cells (DSSCs). The λ_{max} of the metal-to-ligand charge transfer (MLCT) absorption of these four ruthenium dyes (527 nm for **1**, 535 nm for **2**, 585 nm for **3** and 553 nm for **4**) can be tuned by various structural modifications of the ancillary ligand and it was shown that increasing the conjugation length of such ligand reduces the energy as well as the molar absorption coefficient of the MLCT band. The maximum incident photon to current conversion efficiency (IPCE) of 41.4% at 550 nm, 38.6% at 480 nm, 39.4% at 470 nm and 31.1% at 480 nm for **1**-, **2**-, **3**- and **4**-sensitized solar cells were obtained. Respectable power conversion efficiencies of 3.00%, 2.51%, 2.00% and 2.03% were realized, respectively, when the sensitizers **1**, **2**, **3** and **4** were used in DSSCs under the standard air mass (AM) 1.5 sunlight illumination (*versus* 5.9% for standard N719).

Introduction

There is a growing research interest in the design and synthesis of functional materials for applications in molecular devices, memory media and photovoltaic energy conversion.¹⁻⁴ Much attention has been focused on developing photovoltaic device technology and searching for photovoltaic materials and related device architectures.³⁻⁶ Since the first report of a dye-sensitized solar cell (DSSC) by Grätzel and O'Regan in 1991,⁷ DSSCs have attracted considerable research interest due to their low cost, high efficiency, flexible use of materials, and easy fabrication.⁸⁻¹⁴ The best solar-to-electricity conversion efficiency of higher than 10% was achieved by using ruthenium(II) polypyridyl sensitizers, such as **N3**,¹⁵ **N719**,¹⁶ **N907**,¹⁷ and black dye¹⁸ under standard global air mass (AM) 1.5 sunlight. It has been demonstrated that the broad range and high molar absorption coefficient of the metal-to-ligand charge transfer (MLCT) absorption in the visible to near-IR region, as well as the appropriate localization of the frontier orbitals of the ruthenium(II) polypyridyl sensitizers play important roles in achieving higher photovoltaic performance for the energy conversion. The scope and diversity of studies on these ruthenium-based dyes in the realm of practical photovoltaic technology have continued to expand. Attempts have been made to molecularly

engineer the structures of ruthenium complexes to broaden the absorption range, increase the molar absorption coefficient and improve the long-term stability. Since 4,4'-dicarboxylic acid-2,2'-bipyridine (dc bpy) has been shown to be the most widely used anchoring ligand in such ruthenium(II) polypyridyl sensitizers,¹⁹ several heteroleptic ruthenium(II)-polypyridyl sensitizers have been recently reported using highly conjugated ancillary bipyridine ligands, which were modified with light-harvesting chromophores such as thiophene,²⁰ furan,²¹ carbazole²² and thienothiophene moieties,²³ in place of one of the dc bpy anchoring ligands. To date, the majority of work has proliferated exclusively to the use of 4,4'-disubstituted bipyridine derivatives as the ancillary ligands, while research work of the corresponding 5,5'-disubstituted bipyridine congeners was not well elucidated and remains to be largely studied.^{8,24} To advance the development of novel ruthenium-based sensitizers to fill this gap, we have launched an initiative to develop new synthetic routes towards the preparation of a new class of 5,5'-bifunctionalized bipyridine ligands that are capable of affording another family of ruthenium polypyridyl sensitizer dyes for DSSC applications. In fact, the starting precursor 5,5'-dibromo-2,2'-bipyridine^{25,26} itself is synthetically more accessible and hence less costly with a higher synthetic yield as compared to the 4,4'-dibromo-2,2'-bipyridine.^{27,28} While most of the 4,4'-disubstituted-2,2'-bipyridine ancillary ligands were prepared by incorporating the conjugated chromophores and 4,4'-dibromo-2,2'-bipyridine *via* appropriate coupling reactions for the aryl-aryl bond formation, we can do the same to offer some interesting 5,5'-disubstituted-2,2'-bipyridine counterparts in the present study.

In this paper, four new heteroleptic ruthenium(II)-polypyridyl sensitizers, [Ru(dc bpy)(L)(NCS)₂] (L = 5,5'-bis(4-octylthiophen-2-yl)-2,2'-bipyridine (**1**), 5,5'-bis(*N,N*-diphenyl-4-aminophenyl)-2,2'-bipyridine (**2**), 5,5'-bis(5-(*N,N*-diphenyl-4-aminophenyl)-thiophen-2-yl)-2,2'-bipyridine (**3**) and 5,5'-bis(4-octyl-5-(*N,N*-diphenyl-4-aminophenyl)-thiophen-2-yl)-2,2'-bipyridine (**4**))

^aInstitute of Molecular Functional Materials[‡], Department of Chemistry and Centre for Luminescence Materials, Hong Kong Baptist University, Waterloo Road, Kowloon Tong, Hong Kong, P.R. China. E-mail: rwywong@hkbu.edu.hk; Fax: +852 34117348

^bKey Laboratory for Advanced Materials and Institute of Fine Chemicals, East China University of Science and Technology, Meilong Road 130, Shanghai, 200237, P.R. China. E-mail: tianhe@ecust.edu.cn; Fax: +86 21-64252288

† CCDC reference numbers 789721–789723. For crystallographic data in CIF or other electronic format see DOI: 10.1039/c0dt01043j

‡ Areas of Excellence Scheme, University Grants Committee (Hong Kong).

based on 5,5'-disubstituted bipyridine ancillary ligands were synthesized using a one-pot synthetic procedure. This is the first time an ancillary ligand incorporating 5,5'-disubstituted bipyridine unit for ruthenium dyes is presented. Alkylthiophene substituents on the bipyridine moiety are expected to increase the π -conjugation length of the ancillary ligand and influence the photophysical properties of the corresponding ruthenium complexes. The triphenylamine is electron donating in nature and can extend the π -electron delocalization and also facilitate charge transfer.^{29–32} The photophysics and localization of the frontier orbitals of these ruthenium complexes were studied, and the performance of the DSSCs using these complexes as photosensitizers was investigated.

Results and discussion

Syntheses and characterization

The synthetic route for the preparation of the 5,5'-disubstituted-2,2'-bipyridine ligands **L1–L4** is illustrated in Scheme 1. 5,5'-Bis(4-octylthiophen-2-yl)-2,2'-bipyridine (**L1**) and 5,5'-bis(5-(*N,N*-diphenyl-4-aminophenyl)-thiophen-2-yl)-2,2'-bipyridine (**L3**) were synthesized from 5,5'-dibromo-2,2'-bipyridine and tributyl(4-octylthiophen-2-yl)stannane or *N,N*-diphenyl-4-(5-(tributylstannyl)thiophen-2-yl)benzenamine *via* the Stille coupling protocol. The Suzuki coupling reaction of 5,5'-dibromo-2,2'-bipyridine with *N,N*-diphenyl-4-aminophenylboronic acid yielded 5,5'-bis(*N,N*-diphenyl-4-aminophenyl)-2,2'-bipyridine (**L2**). 5,5'-Bis(4-octyl-5-(*N,N*-diphenyl-4-aminophenyl)-thiophen-2-yl)-2,2'-bipyridine (**L4**) was obtained through Suzuki coupling reaction between *N,N*-diphenyl-4-aminophenylboronic acid and 5,5'-bis(4-octyl-5-bromo-thiophen-2-yl)-2,2'-bipyridine, which was prepared by bromination of **L1** with NBS in CHCl_3 .

The heteroleptic ruthenium sensitizers **1–4** were obtained in a typical one pot synthesis from the sequential reaction of ruthenium dimer $[\text{RuCl}_2(p\text{-cymene})_2]$ with each of the newly prepared 5,5'-disubstituted-2,2'-bipyridine ligands, followed by the reaction of the resulting mononuclear complex with 4,4'-dicarboxylic acid-2,2'-bipyridine (dc bpy). The chloro complexes then reacted with an excess of ammonium thiocyanate ligand to afford the target heteroleptic ruthenium complexes **1–4**. The products were purified by chromatography on silica gel. The addition of long octyl chains on the thiophene rings in **4** relative **3** can notably improve the solubility of the dyes in organic solvents as well as to prevent the complexes from water-induced desorption of the dye molecules from the TiO_2 surface.¹²

All of the new organic ligands and their ruthenium complexes were characterized by UV-vis, IR, and ^1H and ^{13}C NMR spectroscopy. The solid-state structures of **L1**, **L2** and **L3** were also

Table 1 Crystallographic data for **L1–L3**

Compound	L1	L2	L3
Formula	$\text{C}_{34}\text{H}_{48}\text{N}_2\text{S}_2$	$\text{C}_{46}\text{H}_{34}\text{N}_4$	$\text{C}_{54}\text{H}_{38}\text{N}_4\text{S}_2$
Formula weight	544.83	642.77	807.00
Crystal system	Triclinic	Monoclinic	Triclinic
Space group	$P\bar{1}$	$C2/c$	$P\bar{1}$
$a/\text{\AA}$	5.5379(4)	14.9729(15)	10.7447(10)
$b/\text{\AA}$	14.5782(11)	25.621(3)	11.8346(11)
$c/\text{\AA}$	19.5515(14)	11.2567(11)	17.2692(16)
$\alpha/^\circ$	107.1120(10)	90	95.596(2)
$\beta/^\circ$	92.4750(10)	128.422(2)	97.058(2)
$\gamma/^\circ$	91.9740(10)	90	108.418(2)
$V/\text{\AA}^3$	1505.32(19)	3383.1(6)	2045.9(3)
Z	2	4	2
T/K	173(2)	173(2)	173(2)
$\mu(\text{Mo-K}\alpha)/\text{mm}^{-1}$	0.202	0.074	0.175
$D(\text{calcd})/\text{g cm}^{-3}$	1.202	1.262	1.310
Total no. of reflections	9521	10474	12904
Unique reflections	6869 (0.0185)	4042	9318 (0.0233)
$[R(\text{int})]$		(0.0299)	
Observed reflections	5758	2535	6845
$[I > 2\sigma(I)]$			
$R_1(F_o)^a$	0.0495	0.0585	0.0445
$wR_2(F_o)^b$	0.1431	0.1609	0.1148
GOF	1.006	1.031	1.015
$\Delta\rho/e \text{\AA}^{-3}$	0.576, -0.781	0.341, -0.222	0.408, -0.312

$$^a R_1 = \sum(|F_o| - |F_c|) / \sum |F_o|. \quad ^b wR_2 = \left\{ \frac{\sum [w(F_o^2 - F_c^2)]}{\sum [w(F_o^2)]} \right\}^{1/2}.$$

determined by single crystal X-ray diffraction. Crystallographic data and structure refinement parameters of **L1–L3** are summarized in Table 1, and ORTEP drawings of **L1**, **L2** and **L3** are depicted in Fig. 1–3, respectively. The ^1H NMR spectra of **1–4** exhibit complicated multiple peaks, which indicate that the dc bpy and 5,5'-disubstituted-2,2'-bipyridine ligands are magnetically non-equivalent. The carboxylic acid protons of the ruthenium complexes were observed at 9.59 and 9.24 ppm for **1**, 9.60 and 9.26 ppm for **2**, 9.72 and 8.58 ppm for **3**, and 9.56 and 9.42 ppm for **4**, respectively, suggesting that the bipyridine ligand contains carboxylic acid groups. FT-IR spectra of **1–4** in KBr pellet show the characteristic intense signal band of the NCS group at around 2100 cm^{-1} , which can be attributed to the *N*-coordinated isothiocyanate group, thus confirming the successful coordination of the NCS moiety to the ruthenium(II) center.

Electronic absorption spectra

The electronic absorption and photoluminescence spectra of the free ligands **L1–L4** in $\text{DMSO}:\text{EtOH} = 2:3$ (v/v) solutions are shown in Fig. 4. They show one or two intense absorption bands in the UV-vis region, which can be assigned to the $\pi \rightarrow \pi^*$ transitions.

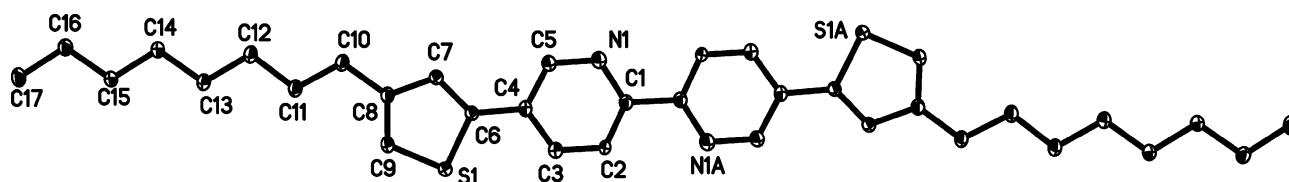
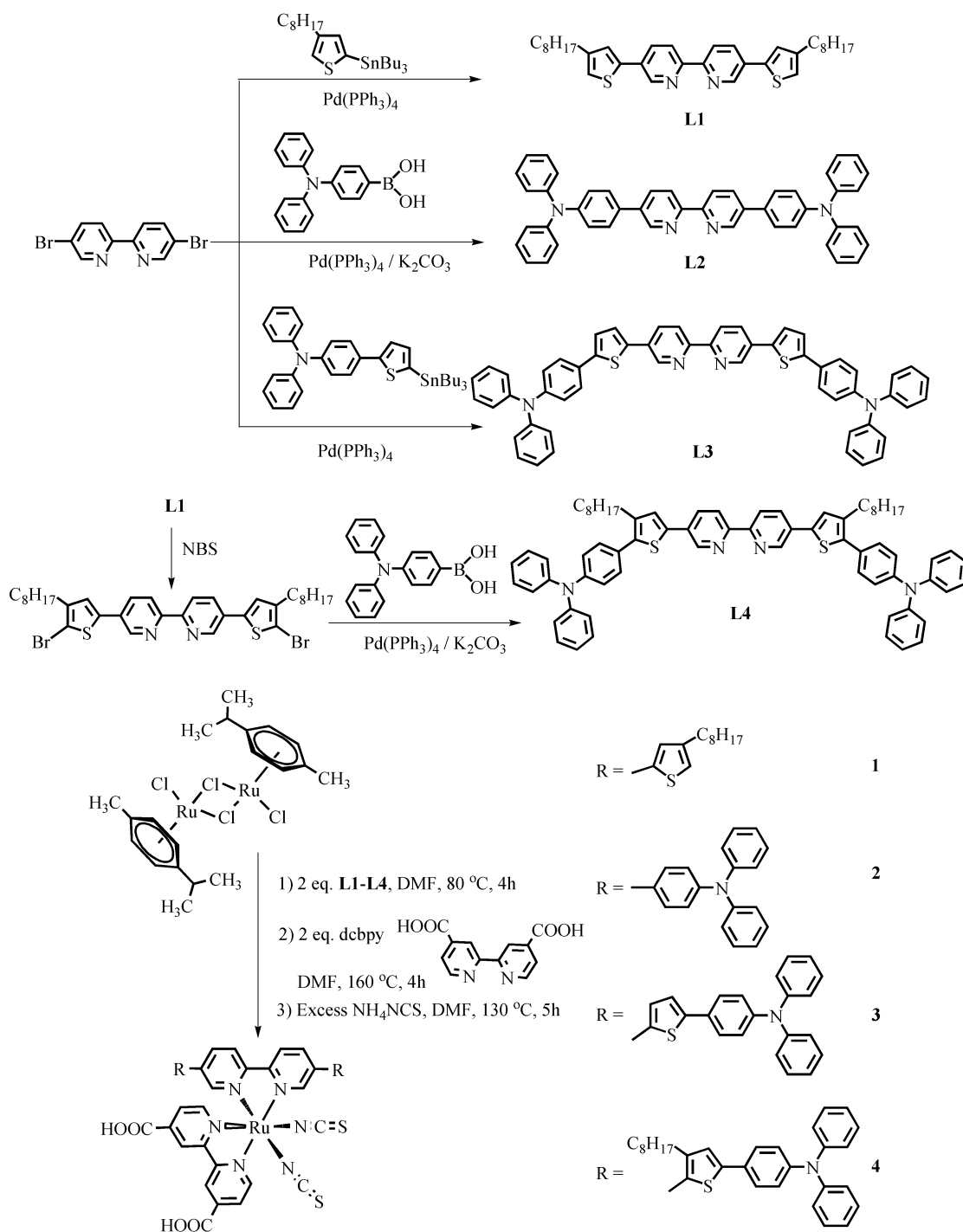


Fig. 1 ORTEP drawing of **L1** with the atom-labeling scheme, showing 30% thermal ellipsoids. Hydrogen atoms are omitted for clarity.



The order of the absorption maximum for these metal-free ligands is **L1** (358 nm) < **L2** (383 nm) < **L4** (399 nm) < **L3** (423 nm), which is partly a manifestation of the increasing conjugated length of the ligands. Comparing **L3** with **L4**, the addition of a large alkyl chain on the thiophene ring would result in a less coplanar configuration for the aromatic rings, making it less conjugated for **L4** than **L3**. The emission maximum of **L1–L4** is centered at 419, 521, 568 and 565 nm, respectively. The emitted light from the ligand may

also offer an additional source of visible light for excitation of the MLCT transition of the corresponding ruthenium complexes.

Fig. 5 shows the UV-vis spectra of the ruthenium complexes **1–4** in DMSO : EtOH = 2 : 3 (v/v) solutions at 293 K, in addition to that of the benchmark compound **N719** used as a reference. The electronic absorption spectral data are summarized in Table 2. The ruthenium complexes show three or four characteristic absorption bands caused by the ligand-centered (LC) electronic transitions

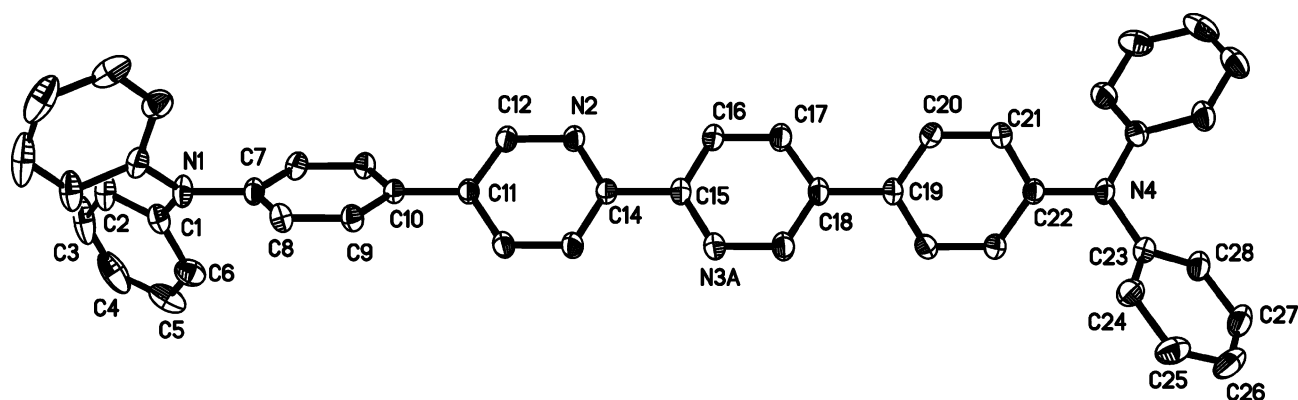


Fig. 2 ORTEP drawing of L2 with the atom-labeling scheme, showing 30% thermal ellipsoids. Hydrogen atoms are omitted for clarity.

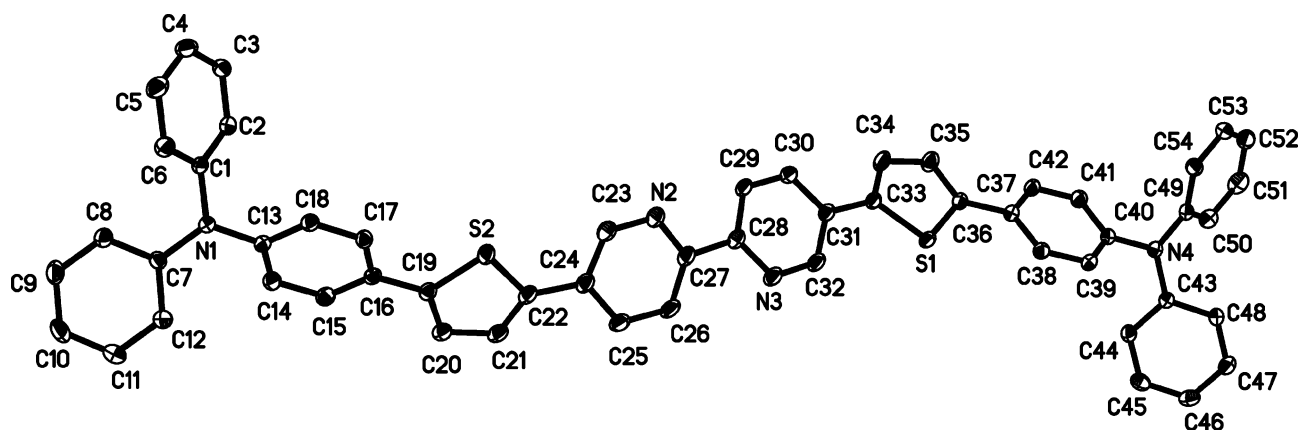


Fig. 3 ORTEP drawing of L3 with the atom-labeling scheme, showing 30% thermal ellipsoids. Hydrogen atoms are omitted for clarity.

Table 2 Absorption and electrochemical data of 1–4 and N719

	λ_{\max}/nm ($\epsilon/10^4 \text{ M}^{-1} \text{ cm}^{-1}$) ^a	HOMO/ eV ^b	LUMO/ eV ^c	E_g/eV^d
1	310 (3.85), 383 (5.55), 527 (0.90)	−5.33	−3.55	1.78
2	305 (5.94), 431 (4.25), 535 (0.64)	−5.66	−3.89	1.77
3	303 (2.34), 353 (2.71), 476 (3.44), 585 (0.32)	−5.46	−3.66	1.80
4	310 (4.11), 343 (2.84), 446 (3.42), 553 (0.59)	−5.64	−3.85	1.79
N719	317 (5.94), 400 (1.75), 541 (1.86)	−5.45 ^e	−3.85 ^e	1.60 ^e

^a Measured in DMSO : EtOH = 2 : 3 (v/v). ^b Calculated from $E_{\text{ox}} - E_{\text{Fc}/\text{Fc}^+} + 4.8$. ^c Calculated from $E_{\text{HOMO}} + E_g$. ^d Optical bandgaps were determined from onset of absorption in DMSO : EtOH = 2 : 3 (v/v). ^e Data from ref. 34.

and/or MLCT transitions. The strong absorption bands centered at 303–353 nm are dominated by LC absorptions due to $\pi \rightarrow \pi^*$ transitions of the bipyridine ligands. The absorption bands with intermediate energy at 383–476 nm can be ascribed to predominant $\pi \rightarrow \pi^*$ LC transitions, mixed with some character from $d \rightarrow \pi^*$ MLCT transitions. These absorption bands result partly from $\pi \rightarrow \pi^*$ LC transitions because the single 5,5'-disubstituted ancillary bipyridines show almost the same absorption pattern. In addition, these absorption bands may be caused by one spin allowed $d \rightarrow \pi^*$ MLCT transitions.³³

The low-energy broad absorption bands centred at 527–585 nm are characteristic of the MLCT transitions from the occupied 4d orbitals of ruthenium to the lowest unoccupied π^* orbitals of the bipyridine ligands in the corresponding ruthenium complexes 1–4. The λ_{\max} of 1–4 in the low-energy region is chemically tunable by structural design and spans a wide absorption range from 527 to 585 nm (*cf.* 541 nm for N719). The absorption wavelength order follows 1 (527 nm) < 2 (535 nm) < 4 (553 nm) < 3 (585 nm), which is in line with the increasing conjugation length of the 5,5'-disubstituted ancillary bipyridines L1–L4 (*vide supra*). In contrast, the molar absorption coefficient for the MLCT band of these ruthenium dyes displays the order 1 (9000 $\text{M}^{-1} \text{ cm}^{-1}$) > 2 (6400 $\text{M}^{-1} \text{ cm}^{-1}$) > 4 (5900 $\text{M}^{-1} \text{ cm}^{-1}$) > 3 (3200 $\text{M}^{-1} \text{ cm}^{-1}$), which are smaller than that of N719 (18600 $\text{M}^{-1} \text{ cm}^{-1}$). These results indicate that increasing the conjugation length of the ancillary ligand can lower the MLCT energy, but also decrease the absorption intensity of the MLCT transition.

Although the molar absorption coefficients for the MLCT bands of 1–4 are lower than those of the state-of-the-art dyes N719 (*cis*-di(thiocyanato)bis(2,2'-bipyridine-4,4'-dicarboxylate)ruthenium(II) bis(tetrabutylammonium) salt (18600 $\text{M}^{-1} \text{ cm}^{-1}$ at 541 nm) and CYC-B3 (*cis*-di(thiocyanato)-4,4'-di(octylthienyl)-2,2'-bipyridine-4,4'-carboxylic acid-2,2'-bipyridine ruthenium(II))^{20e} (15700 $\text{M}^{-1} \text{ cm}^{-1}$ at 544 nm in DMF), the light-harvesting ability of 1–4 in the intermediate energy region appears higher than those of the dyes N719 and CYC-B3.

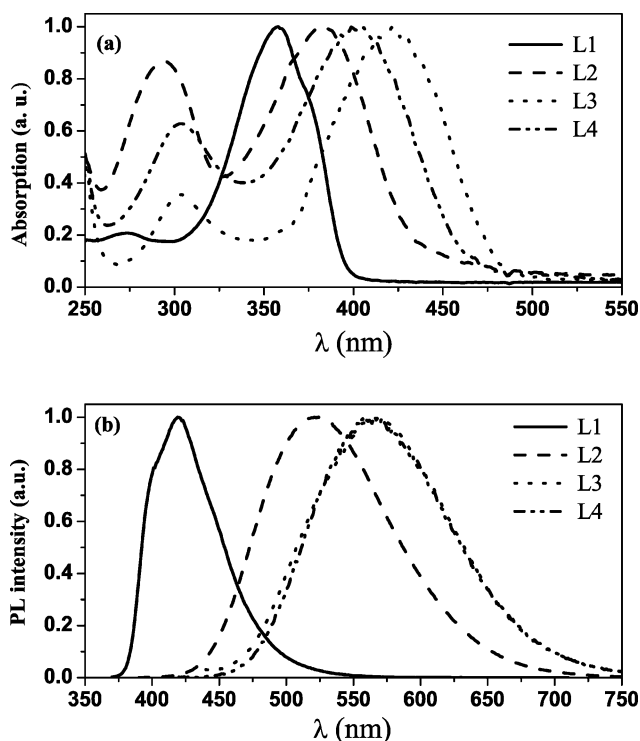


Fig. 4 (a) Normalized absorption and (b) photoluminescence spectra of L1–L4 in DMSO : EtOH = 2 : 3 (v/v) at 293 K.

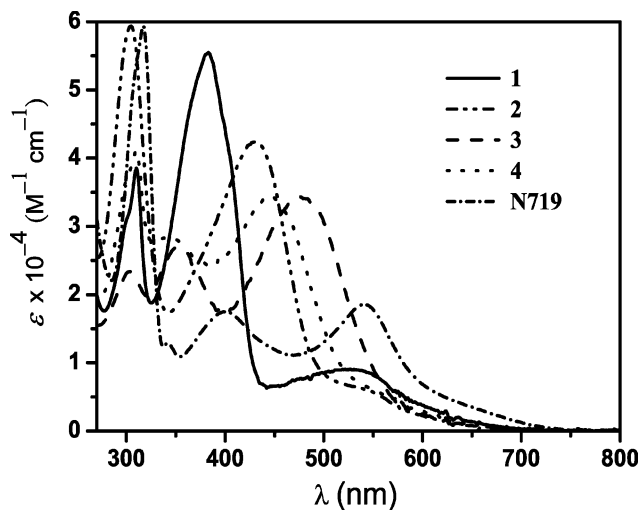


Fig. 5 UV-vis absorption spectra of 1–4 and N719 in DMSO : EtOH = 2 : 3 (v/v).

Electrochemistry

To evaluate the possibility of electron transfer from the excited dye molecule to the conductive band (E_{cb}) of TiO_2 , oxidative cyclic voltammetry was performed in the acetonitrile solvent using 0.1 M tetrabutylammonium hexafluorophosphate as the supporting electrolyte, TiO_2 films stained with sensitizer as the working electrode, Pt as the counter electrode and saturated calomel electrode (SCE) as the reference electrode. Under these conditions, the $E_{1/2}$ of ferrocene was 0.37 V vs. SCE.

The band structures of 1–4, which should match the energy level of the semiconductor anode and the redox electrolyte, can

be established from the electrochemical and absorption data. As shown in Fig. 6, the oxidation of all complexes is irreversible since the oxidation potential of the thiocyanate ligand is close to that for Ru(II), as observed for other related ruthenium dyes.^{19,35} The Ru(III/II) oxidation potential of 1, 2, 3 and 4 were found to be 0.90, 1.23, 1.03, and 1.21 (V vs. SCE), respectively, which are higher than the I^-/I_3^- electrolyte (0.5 V), ensuring effective sensitizer regeneration process.³⁶ The Ru(III/II) oxidation potential order $1 < 4$ can be rationalized from the increased degree of conjugation in the presence of electron-releasing triphenylamino. The corresponding order $3 < 4$ is caused by the increased electron richness of the bipyridyl ligand in 4 due to the presence of an electron-releasing octyl substituent, rendering the Ru(II) center less susceptible to oxidation in 4. The LUMO levels of these sensitizers are all much higher than the lower bound of the conduction band of TiO_2 (–4.4 eV), indicating that the efficiency of charge injection from the excited sensitizer molecule to the TiO_2 conduction band is viable.³⁶ The energy level diagrams of 1–4, N719, TiO_2 , and the I^-/I_3^- redox couple are depicted in Fig. 7.

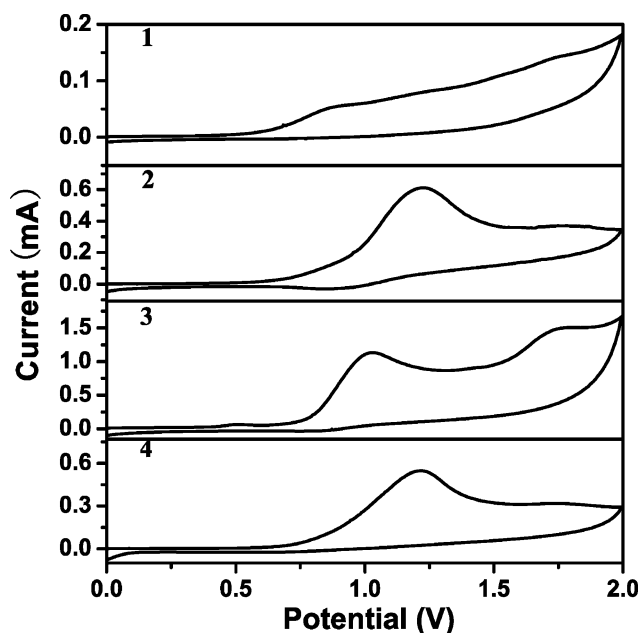


Fig. 6 Oxidative cyclic voltammetry of the photosensitizers adsorbed on the electrode coated with a thin layer of TiO_2 .

Computational studies

The geometry optimization, electronic structure and localization of the frontier orbitals of complexes 1–4 were carried out by the density functional theory (DFT) calculations based on the Becke's three parameters employing Lee-Yang-Parr exchange functional (B3LYP) with 6-31G* basis sets. As shown from the orbital profiles in Fig. 8, the components of the frontier orbitals of 1–4 are similar to each other. The highest occupied molecular orbitals, HOMO and HOMO-1, of the four ruthenium dyes are mainly located at the ruthenium metal and the NCS ligands, in which the ruthenium metal character is about 11–19% and the NCS ligand character is about 74–86%. Within the NCS ligands, the amplitude is located on the sulfur atom. The lowest unoccupied molecular orbitals (LUMO) of 1–4 have amplitudes mostly on the anchoring ligands

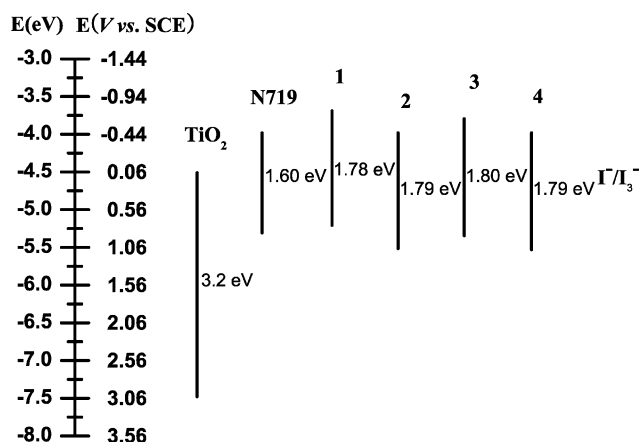


Fig. 7 Energy level diagrams of 1–4, N719, TiO₂, and I⁻/I₃⁻.

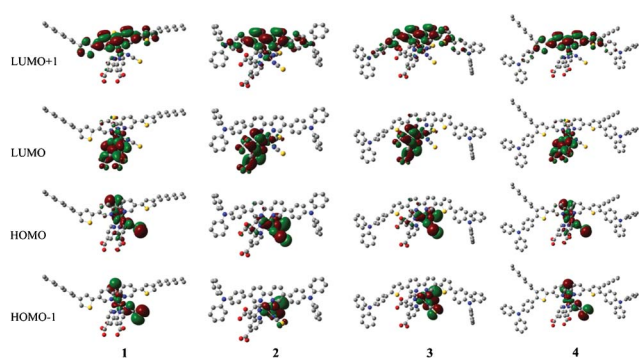


Fig. 8 Contour plots of selected frontier orbitals of 1–4.

(dcbpy) that can facilitate electron injection from the excited metal complex to TiO₂, while the LUMO+1 is mainly located on the ancillary bipyridine ligands. It was revealed that the HOMO–LUMO excitation transferred the electrons from the NCS ligands to the anchoring ligands (dcbpy), and the photoinduced electron injection from the dye to TiO₂ can be efficiently mediated by the HOMO–LUMO transition.

Performance of dye-sensitized solar cells

The photocurrent action spectra of DSSCs with sensitizers 1–4 are presented in Fig. 9. Considering the incident photon to current conversion efficiency (IPCE) of these ruthenium dyes, the IPCE curves cover almost the entire visible spectrum with a maximum of IPCE values of 41.4% at 550 nm, 38.6% at 480 nm, 39.4% at 470 nm and 31.1% at 480 nm for 1-, 2-, 3- and 4-sensitized solar cells, respectively.

The short-circuit photocurrent density (J_{sc}), open-circuit photovoltage (V_{oc}), and fill factor (ff) of the DSSCs were measured under standard AM 1.5 sunlight illumination. The photocurrent-voltage curves for DSSCs based on sensitizers 1–4 are shown in Fig. 10 and the detailed device performance data are listed in Table 3. The J_{sc} of the solar cells with 1, 2, 3 and 4 are 6.56, 5.60, 4.93 and 4.49 mA cm⁻², respectively. These values are lower than that of the optimized solar cells with N719 dye (13.81 mA cm⁻²), and the difference can be attributed to the notion that MLCT molar extinction coefficients of 1–4 are lower than that of N719 in solution (*vide supra*). The power conversion efficiency (η) of 1-, 2-, 3- and 4-sensitized solar cells are moderate at 3.00%, 2.51%,

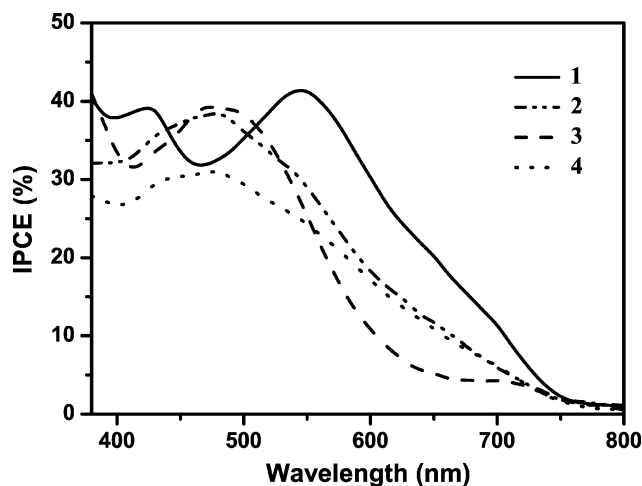


Fig. 9 Photocurrent action spectra of the TiO₂ electrode sensitized by 1–4.

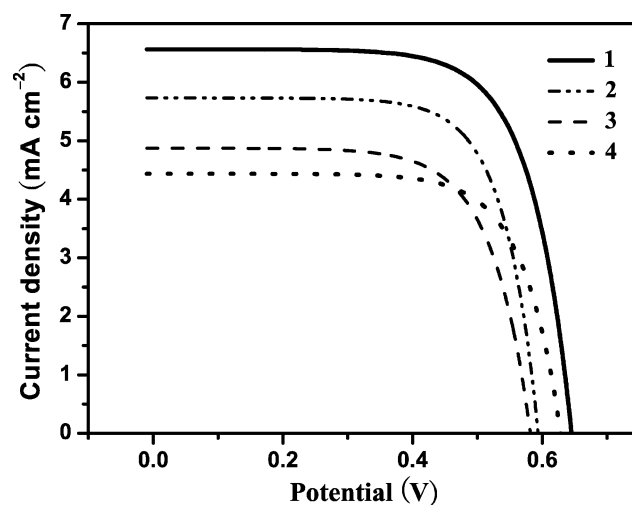


Fig. 10 Photocurrent-voltage curves for DSSCs based on photosensitizers 1–4.

2.00% and 2.03%, respectively (*vs.* 5.9% for N719 under the same device-fabrication process and measuring parameters). The lower η is largely due to the lower J_{sc} (or molar extinction coefficient) of the sensitizers as compared to N719 that is associated with their weaker light-harvesting capacity and bulky molecular structures, although the ff of the present devices are all slightly higher than that for N719. The values of the devices are consistent with the MLCT band absorption coefficient of the photosensitizers.

Table 3 Photovoltaic performance of DSSCs with different 1-, 2-, 3- and 4- and N719-sensitizers under the AM 1.5 sunlight

	$J_{sc}/\text{mA cm}^{-2}$	V_{oc}/mV	ff	η (%)
1	6.56	649	0.70	3.00
2	5.60	592	0.76	2.51
3	4.93	584	0.69	2.00
4	4.49	633	0.71	2.03
N719	13.81	657	0.65	5.9

Concluding remarks

A series of heteroleptic ruthenium complexes containing uncommon 5,5'-disubstituted-2,2'-bipyridine ancillary ligands were synthesized and fully characterized by spectroscopic and DFT studies. The different substituent on bipyridine acts as a good functional chromophore to tune the overall properties of the complex. The relationship between the nature of the ancillary ligand and the DSSC performance of the dye was investigated. As demonstrated by the absorption spectral studies, the increase in conjugation length of the ancillary ligand results in a lower MLCT energy and a diminished intensity of the transition. Photosensitizer **1** gave the highest conversion efficiency of 3.00%, and among **1–4**, the performance results correlate well with the molar absorption coefficient of the MLCT band of the dyes and their different light-harvesting ability. These findings suggest that bipyridine chromophores substituted at the synthetically more accessible 5,5'-positions opens an alternative good class of ancillary ligands over the traditional 4,4'-disubstituted ones for use in DSSC research based on the photosensitizing metal polypyridyl core. Work is still underway for device optimization and it is possible to gain higher efficiencies with a thicker TiO₂ film.

Experimental

Materials and reagents

All manipulations were performed under dry nitrogen atmosphere by using Schlenk techniques. Solvents were dried by standard methods and distilled prior to use. Di- μ -chlorobis[(η^6 -*p*-cymene)chlororuthenium(II)] ([RuCl₂(*p*-cymene)]₂) was purchased from Strem Chemical Inc. (USA). **N719** dye was purchased from Solaronix SA Co. (Switzerland). 4,4'-Dicarboxylic acid-2,2'-bipyridine (dc bpy) was prepared according to the reported procedure in the literature.³⁷ 5,5'-Dibromo-2,2'-bipyridine,²⁵ tributyl(4-octylthiophen-2-yl)stannane,³⁸ *N,N*-diphenyl-4-aminophenylboronic acid³⁹ and *N,N*-diphenyl-4-(5-(tributylstannyl)thiophen-2-yl)benzenamine⁴⁰ were prepared according to the published method, and other chemicals are commercially available and used as received.

Physical measurements

Infrared spectra were recorded as KBr pellets using a Perkin-Elmer Paragon 1000 PC or Nicolet Magna 550 Series II FTIR spectrometer. MALDI-TOF mass spectra were measured on an Autoflex Bruker MALDI-TOF MS instrument. NMR spectra were measured in CDCl₃ or DMSO-*d*₆ on a Bruker AM 400 MHz FT-NMR spectrometer, and chemical shifts were quoted relative to tetramethylsilane for ¹H and ¹³C nuclei. UV-Vis spectra were obtained on a HP-8453 diode array spectrophotometer.

DFT computational method

All calculations were performed using the Gaussian 03 program package.⁴¹ The B3LYP (Becke-3-Lee-Yang-Par)⁴² DFT method was chosen because of its high accuracy and it is not computationally demanding. The LAN2DZ basis set was applied for Ru and S atoms, and 6-31G* basis set was employed for C, H, N and O atoms.

X-Ray crystallography†

X-Ray diffraction data were collected at 173 K using graphite-monochromated Mo-K α radiation ($\lambda = 0.71073$ Å) on a Bruker Axs SMART 1000 CCD diffractometer. The collected frames were processed with the software SAINT⁴³ and an absorption correction (SADABS)⁴⁴ was applied to the collected reflections. The structure was solved by the Direct method (SHELXTL)⁴⁵ in conjunction with standard difference Fourier techniques and subsequently refined by full-matrix least-squares analyses on F^2 . Hydrogen atoms were generated in their idealized positions and all non-hydrogen atoms were refined anisotropically.

Fabrication of photovoltaic devices

A screen-printed double layer of TiO₂ particles was used as photoelectrodes. A 10 μ m thick film of 13 nm-sized TiO₂ particles (Ti-Nanoxide T/SP) was first printed on the FTO conducting glass and further coated by a 4 μ m thick second layer of 400 nm light-scattering anatase particles (Ti-Nanoxide 300). Sintering was carried out at 450 °C for 30 min. Before immersion in the dye solution, these films were immersed into a 40 mM aqueous TiCl₄ solution at 70 °C for 30 min and washed with water and ethanol. Then the films were heated again at 450 °C for 30 min followed by cooling to 80 °C and dipping into a 3×10^{-4} M solution of dyes in DMSO : EtOH = 2 : 3 (v/v) for 12 h at room temperature. Chenodeoxycholic acid (CDCA) as a coadsorbent was adsorbed on the TiO₂ films in a 3×10^{-4} M CDCA in acetonitrile solution for 0.5 h or 1 h before dipping into the solution of dyes. To prepare the counter electrode, the Pt catalyst was deposited on the cleaned FTO glass by coating the FTO with a drop of H₂PtCl₆ solution (0.02 M in 2-propanol solution) with the heat treatment at 400 °C for 15 min. A hole (0.8 mm diameter) was drilled on the counter electrode by a Drill-press. The perforated sheet was cleaned by ultrasound in an ethanol bath for 10 min. About the assemblage of DSSCs, the dye-covered TiO₂ electrode and Pt-counter electrode were assembled into a sandwich type cell and sealed with a hot-melt gasket of 25 μ m thickness made of the ionomer Surlyn 1702 (Dupont). The size of the TiO₂ electrodes used was 0.25 cm² (*i.e.*, 5 mm \times 5 mm). A drop of the electrolyte was put on the hole in the back of the counter electrode. It was introduced into the cell *via* vacuum backfilling. The hole in the counter electrode was sealed by a film of Surlyn 1702 and a cover glass (0.1 mm thickness) using a hot iron bar.

DSSC measurements

Photovoltaic measurements employed an AM 1.5 solar simulator equipped with a 1000 W xenon lamp (Model No. 91160, Oriel). The power of the simulated light was calibrated to 100 mW cm⁻² using a Newport Oriel PV reference cell system (Model 91150V). *J–V* curves were obtained by applying an external bias to the cell and measuring the generated photocurrent with a Keithley model 2400 digital source meter. The voltage step and delay time of photocurrent were 10 mV and 40 ms, respectively. Cell active area was tested with a mask of 0.158 cm². The photocurrent action spectra were measured with an IPCE test system consisting of a Model SR830 DSP lock-in amplifier and a Model SR540 optical chopper (Stanford Research Corporation, USA), a 7IL/PX150 xenon lamp and power supply, and a 7ISW301 spectrometer.

Impedance spectra were done using a CHI-660c electrochemical station.

Synthesis

5,5'-Bis(4-octylthiophen-2-yl)-2,2'-bipyridine (L1). 5,5'-Dibromo-2,2'-bipyridine (0.32 g, 1.00 mmol), tributyl(4-octylthiophen-2-yl)stannane (1.1 g, 2.25 mmol) and Pd(PPh₃)₄ (0.116 g, 0.10 mmol, 5 mol%) were dissolved in dry toluene (30 mL) and the mixture was refluxed under N₂ for two days. After evaporation of the solvent under reduced pressure, the resulting solid was purified by column chromatography on silica gel using CH₂Cl₂ as eluent to afford **L1** as a yellow solid (0.41 g, 0.75 mmol, 75%). ¹H NMR (400 MHz, CDCl₃): δ = 8.91 (s, 2H, Ar), 8.40 (d, *J* = 8.3 Hz, 2H, Ar), 7.97 (d, *J* = 8.3 Hz, 2H, Ar), 7.26 (s, 2H, Ar), 6.97 (s, 2H, Ar), 2.66–2.62 (m, 4H, alkyl), 1.68–1.64 (m, 4H, alkyl), 1.36–1.28 (m, 20H, alkyl), 0.90–0.87 (m, 6H, alkyl) ppm. ¹³C NMR (100 MHz, CDCl₃): δ = 154.23, 146.10, 144.75, 139.97, 133.43, 130.44, 125.66, 120.86, 120.84 (Ar), 31.89, 30.56, 30.47, 29.44, 29.34, 29.27, 22.68, 14.13 (alkyl) ppm. MS (MALDI-TOF): *m/z* = 545.29 (M+H)⁺. Anal. calc. for C₃₄H₄₄N₂S₂: C, 74.95; H, 8.14; N, 5.14. Found: C, 75.10; H, 8.20; N, 5.25.

5,5'-Bis(*N,N*-diphenyl-4-aminophenyl)-2,2'-bipyridine (L2). To a solution of 5,5'-dibromo-2,2'-bipyridine (0.33 g, 1.05 mmol), *N,N*-diphenyl-4-aminophenylboronic acid (0.87 g, 3.00 mmol) and Pd(PPh₃)₄ (0.116 g, 0.10 mmol, 5 mol%) in a mixture of toluene (10 mL) and THF (20 mL) was added a solution of K₂CO₃ (2 M, 4 mL). The reaction mixture was stirred under reflux for two days. After evaporation of the solvent under reduced pressure, water (50 mL) and dichloromethane (50 mL) were added. The organic layer was separated, washed with water and brine, and dried over anhydrous Na₂SO₄. The solvent was removed under reduced pressure, and the crude product was purified by column chromatography on silica gel with dichloromethane–ethyl acetate = 10 : 1 (v/v) as the eluent to afford **L2** as an orange solid in 68% yield (0.44 g, 0.68 mmol). ¹H NMR (400 MHz, CDCl₃): δ = 8.91 (s, 2H, Ar), 8.46 (d, *J* = 8.2 Hz, 2H, Ar), 8.00 (d, *J* = 8.3 Hz, 2H, Ar), 7.55–7.53 (m, 4H, Ar), 7.27–7.31 (m, 8H, Ar), 7.19–7.14 (m, 12H, Ar), 7.09–7.05 (m, 4H, Ar) ppm. ¹³C NMR (100 MHz, CDCl₃): δ = 154.09, 148.10, 147.40, 147.18, 135.82, 134.54, 130.90, 129.38, 127.66, 124.75, 123.51, 123.34, 120.89 (Ar) ppm. MS (MALDI-TOF): *m/z* = 643.17 (M+H)⁺. Anal. calc. for C₄₆H₃₄N₄: C, 85.95; H, 5.33; N, 8.72. Found: C, 86.10; H, 5.15; N, 8.98.

5,5'-Bis(5-(*N,N*-diphenyl-4-aminophenyl)-thiophen-2-yl)-2,2'-bipyridine (L3). The procedure described for the synthesis of **L1** was followed to produce **L3** from *N,N*-diphenyl-4-(5-(tributylstannyl)thiophen-2-yl)benzenamine (0.92 g, 1.50 mmol) and 5,5'-dibromo-2,2'-bipyridine (0.21 g, 0.67 mmol). The crude product was purified by column chromatography on silica gel eluting with dichloromethane–ethyl acetate = 10 : 1 (v/v) to yield 0.40 g of the product as an orange solid (0.49 mmol, 73%). ¹H NMR (400 MHz, CDCl₃): δ = 8.94 (s, 2H, Ar), 8.43 (d, *J* = 8.3 Hz, 2H, Ar), 7.99 (d, *J* = 8.3 Hz, 2H, Ar), 7.52–7.49 (m, 4H, Ar), 7.41–7.40 (m, 2H, Ar), 7.30–7.24 (m, 10H, Ar), 7.15–7.13 (m, 8H, Ar), 7.10–7.04 (m, 8H, Ar) ppm. ¹³C NMR (100 MHz, CDCl₃): δ = 154.11, 147.66, 147.36, 145.90, 145.12, 138.51, 133.10, 130.23, 129.36, 127.75, 126.54, 125.29, 124.66, 123.41, 123.33, 123.28,

120.89 (Ar) ppm. MS (MALDI-TOF): *m/z* = 807.31 (M+H)⁺. Anal. calc. for C₅₄H₃₈N₄S₂: C, 80.37; H, 4.75; N, 6.94. Found: C, 80.55; H, 4.86; N, 7.08.

5,5'-Bis(4-octyl-5-(*N,N*-diphenyl-4-aminophenyl)-thiophen-2-yl)-2,2'-bipyridine (L4). A solution of **L1** (0.41 g, 0.75 mmol) in chloroform (15 ml) was stirred and cooled to 0 °C. *N*-Bromosuccinimide (NBS) (0.14 g, 0.75 mmol) was added in small portions. After stirring overnight at room temperature, the reaction mixture was poured into water. The organic phase was separated and dried over anhydrous Na₂SO₄. After the solvent was evaporated, the crude product was purified by recrystallization from methanol to afford 5,5'-bis(4-octyl-5-bromo-thiophen-2-yl)-2,2'-bipyridine in 87% yield (0.46 g, 0.65 mmol). ¹H NMR (400 MHz, CDCl₃): δ = 8.84 (s, 2H, Ar), 8.40 (d, *J* = 8.3 Hz, 2H, Ar), 7.90 (d, *J* = 8.3 Hz, 2H, Ar), 7.13 (s, 2H, Ar), 2.61–2.57 (m, 4H, alkyl), 1.63–1.60 (m, 4H, alkyl), 1.36–1.28 (m, 20H, alkyl), 0.90–0.87 (m, 6H, alkyl) ppm. ¹³C NMR (100 MHz, CDCl₃): δ = 154.37, 145.80, 143.64, 139.56, 133.20, 129.83, 125.29, 121.00, 109.90 (Ar), 31.89, 29.74, 29.66, 29.58, 29.39, 29.26, 22.68, 14.14 (alkyl) ppm.

The procedure described for the synthesis of **L2** was followed to produce **L4** from *N,N*-diphenyl-4-aminophenylboronic acid (0.44 g, 1.50 mmol) and 5,5'-bis(4-octyl-5-bromo-thiophen-2-yl)-2,2'-bipyridine (0.35 g, 0.50 mmol). The crude product was purified by column chromatography on silica gel with dichloromethane–ethyl acetate = 50 : 1 (v/v) as eluent to give 0.36 g of the product as an orange solid (0.35 mmol, 70%). ¹H NMR (400 MHz, CDCl₃): δ = 8.90 (s, 2H, Ar), 8.38 (d, *J* = 8.3 Hz, 2H, Ar), 7.93 (d, *J* = 8.3 Hz, 2H, Ar), 7.32–7.24 (m, 14H, Ar), 7.15–7.13 (m, 8H, Ar), 7.09–7.07 (m, 4H, Ar), 7.05–7.01 (m, 4H, Ar), 2.69–2.64 (m, 4H, alkyl), 1.66–1.63 (m, 4H, alkyl), 1.32–1.20 (m, 20H, alkyl), 0.90–0.87 (m, 6H, alkyl) ppm. ¹³C NMR (100 MHz, CDCl₃): δ = 154.06, 147.50, 147.35, 145.87, 139.63, 138.96, 137.44, 132.99, 130.26, 129.85, 129.42, 127.86, 126.91, 124.80, 123.30, 122.95, 120.87 (Ar), 31.97, 31.10, 29.63, 29.49, 29.35, 28.99, 22.76, 14.24 (alkyl) ppm. MS (MALDI-TOF): *m/z* = 1031.62 (M+H)⁺. Anal. calc. for C₇₀H₇₀N₄S₂: C, 81.51; H, 6.84; N, 5.43. Found: C, 81.76; H, 6.80; N, 5.28.

General procedure for the synthesis of the ruthenium sensitizers

In a typical one-pot synthesis, [RuCl₂(*p*-cymene)]₂ (138 mg, 0.23 mmol) was dissolved in dry DMF (25 mL) and the respective 5,5'-disubstituted-2,2'-bipyridine ligand (**L1**, **L2**, **L3** or **L4**, 0.45 mmol) was added. The reaction mixture was stirred at 80 °C under argon for 4 h and then dcbpy (110 mg, 0.45 mmol) was added. The reaction mixture was refluxed at 160 °C for another 4 h in the dark to avoid the photoinduced *cis*-to-*trans* isomerization. After addition of excess NH₄NCS (330 mg, 4.50 mmol), the reaction mixture was stirred at 130 °C for 5 h. After the reaction, the solvent was removed by using a rotary evaporator. Then, water was added to the resulting mixture to remove any excess NH₄NCS. The water-insoluble product was collected, washed with distilled water, followed by diethyl ether, and dried in air. Purification of the crude product was achieved by column chromatography on silica gel using chloroform–methanol (2 : 1, v/v) as the eluent. The main band was collected and a few drops of 0.01 M HNO₃(aq) was added. One to four successive chromatographic separation was necessary to ensure the desired purity.

[Ru(dcbpy)(L1)(NCS)₂] (1). Purple solid. ¹H NMR (400 MHz, DMSO-*d*₆): δ = 9.59 (s, 1H, Ar), 9.24 (s, 1H, Ar), 8.87 (s, 1H, Ar), 8.76 (d, *J* = 8.7 Hz, 2H, Ar), 8.68 (s, 1H, Ar), 8.61 (d, *J* = 8.5 Hz, 1H, Ar), 8.46 (d, *J* = 8.0 Hz, 1H, Ar), 8.21–8.18 (m, 2H, Ar), 7.88 (s, 1H, Ar), 7.65 (s, 1H, Ar), 7.52–7.42 (m, 5H, Ar), 7.23–7.20 (m, 1H, Ar), 1.66 (m, 2H, alkyl), 1.49 (m, 2H, alkyl), 1.31–1.21 (m, 24H, alkyl), 0.85–0.81 (m, 6H, alkyl) ppm. IR (KBr) (cm⁻¹): 2103 s (NCS). MS (MALDI-TOF): *m/z* = 1043.24 (M+2H₂O+H)⁺, 948.29 (M-NCS)⁺. Anal. calc. for C₄₈H₅₂N₆O₄S₄Ru: C, 57.29; H, 5.21; N, 8.35. Found: C, 57.40; H, 5.25; N, 8.56.

[Ru(dcbpy)(L2)(NCS)₂] (2). Black solid. ¹H NMR (400 MHz, DMSO-*d*₆): δ = 9.60 (s, 1H, Ar), 9.26 (s, 1H, Ar), 8.82–8.80 (m, 2H, Ar), 8.67–8.65 (m, 2H, Ar), 8.53 (d, *J* = 8.4 Hz, 1H, Ar), 8.16–8.11 (m, 2H, Ar), 7.94 (d, *J* = 8.6 Hz, 1H, Ar), 7.64–7.53 (m, 4H, Ar), 7.40–7.31 (m, 10H, Ar), 7.25–7.23 (m, 2H, Ar), 7.15–7.10 (m, 10H, Ar), 7.04–7.02 (m, 4H, Ar), 6.86–6.84 (m, 2H, Ar) ppm. IR (KBr) (cm⁻¹): 2099 s (NCS). MS (MALDI-TOF): *m/z* = 1141.28 (M+2H₂O+H)⁺, 1046.35 (M-NCS)⁺. Anal. calc. for C₆₀H₄₂N₈O₄S₂Ru: C, 65.26; H, 3.83; N, 10.15. Found: C, 65.53; H, 3.98; N, 10.24.

[Ru(dcbpy)(L3)(NCS)₂] (3). Black solid. ¹H NMR (400 MHz, DMSO-*d*₆): δ = 9.72 (s, 1H, Ar), 8.75 (d, *J* = 8.5 Hz, 1H, Ar), 8.57 (d, *J* = 8.4 Hz, 2H, Ar), 8.21 (d, *J* = 8.2 Hz, 1H, Ar), 8.00 (d, *J* = 3.7 Hz, 1H, Ar), 7.64 (s, 1H, Ar), 7.60 (d, *J* = 3.2 Hz, 1H, Ar), 7.55 (d, *J* = 3.7 Hz, 1H, Ar), 7.47 (d, *J* = 8.6 Hz, 2H, Ar), 7.38–7.26 (m, 12H, Ar), 7.10–6.96 (m, 20H, Ar), 6.87–6.85 (m, 3H, Ar) ppm. IR (KBr) (cm⁻¹): 2094 s (NCS). MS (MALDI-TOF): *m/z* = 1210.19 (M-NCS)⁺. Anal. calc. for C₆₈H₄₆N₈O₄S₄Ru: C, 64.39; H, 3.66; N, 8.83. Found: C, 64.54; H, 3.98; N, 8.60.

[Ru(dcbpy)(L4)(NCS)₂] (4). Black solid. ¹H NMR (400 MHz, DMSO-*d*₆): δ = 9.56 (s, 1H, Ar), 9.42 (s, 1H, Ar), 9.05 (s, 1H, Ar), 8.86 (s, 1H, Ar), 8.66 (s, 1H, Ar), 8.50 (s, 1H, Ar), 8.34 (s, 1H, Ar), 8.29 (s, 1H, Ar), 7.95 (s, 1H, Ar), 7.90 (s, 1H, Ar), 7.39 (d, *J* = 8.2 Hz, 2H, Ar), 7.35–7.30 (m, 10H, Ar), 7.22 (d, *J* = 8.4 Hz, 2H, Ar), 7.12–7.00 (m, 18H, Ar), 6.96–6.94 (d, 2H, Ar), 1.66 (s, 4H, alkyl), 1.44 (s, 4H, alkyl), 1.23–1.20 (m, 20H, alkyl), 0.82–0.81 (m, 6H, alkyl) ppm. IR (KBr) (cm⁻¹): 2104 s (NCS). MS (MALDI-TOF): *m/z* = 1529.42 (M+2H₂O+H)⁺, 1434.41 (M-NCS)⁺. Anal. calc. for C₈₄H₇₈N₈O₄S₄Ru: C, 67.58; H, 5.27; N, 7.51. Found: C, 67.66; H, 5.40; N, 7.78.

Acknowledgements

This work has been supported by the University Grants Committee Areas of Excellence Scheme (AoE/P-03/08) and the Hong Kong Baptist University. We also thank the National Science Foundation of China (NSFC) (project number: 21029001) for financial support.

References

- 1 B. L. Feringa, *Molecular Switches*, Wiley-VCH, Weinheim, 2001.
- 2 V. Balzani, M. Venturi and A. Credi, *Molecular Devices and Machines*, Wiley-VCH, Weinheim, 2003.
- 3 (a) W.-Y. Wong and C.-L. Ho, *Coord. Chem. Rev.*, 2009, **253**, 1709–1758; (b) W.-Y. Wong and C.-L. Ho, *J. Mater. Chem.*, 2009, **19**, 4457–4482; (c) Y. Chi and P.-T. Chou, *Chem. Soc. Rev.*, 2010, **39**, 638–655; (d) Y.-J. Cheng, S.-H. Yang and C.-S. Hsu, *Chem. Rev.*, 2009, **109**, 5868–5923; (e) S. Gunes, H. Neugebauer and N. S. Sariciftci, *Chem. Rev.*, 2007, **107**, 1324–1338; (f) B. C. Thompson and J. M. Frechet, *Angew. Chem., Int. Ed.*, 2008, **47**, 58–77.
- 4 G. Vilaca, B. Jousseau, C. Mahieux, C. Belin, H. Cachet, M. C. Bernard, V. Vivier and T. Toupance, *Adv. Mater.*, 2006, **18**, 1073–1077.
- 5 (a) B. C. O'Regan and J. R. Durrant, *Acc. Chem. Res.*, 2009, **42**, 1799–1808; (b) W.-Y. Wong and C.-L. Ho, *Acc. Chem. Res.*, 2010, **43**, 1246–1256.
- 6 W.-Y. Wong, *Macromol. Chem. Phys.*, 2008, **209**, 14–24.
- 7 B. O'Regan and M. Grätzel, *Nature*, 1991, **353**, 737–740.
- 8 S. Ardo and G. J. Meyer, *Chem. Soc. Rev.*, 2009, **38**, 115–164.
- 9 (a) M. Grätzel, *Acc. Chem. Res.*, 2009, **42**, 1788–1798; (b) M. K. Nazeeruddin and M. Grätzel, *Struct. Bonding*, 2007, **123**, 113–175; (c) L. M. Gonçalves, V. de Zea Bermudez, H. A. Ribeiro and A. M. Mendes, *Energy Environ. Sci.*, 2008, **1**, 655–667.
- 10 M. Grätzel, *Nature*, 2001, **414**, 338–344.
- 11 A. Hagfeldt and M. Grätzel, *Acc. Chem. Res.*, 2000, **33**, 269–277.
- 12 N. Robertson, *Angew. Chem., Int. Ed.*, 2006, **45**, 2338–2345.
- 13 M. K. Nazeeruddin and M. Grätzel in *Comprehensive Coordination Chemistry II*, Vol. 9 (ed., J. A. McCleverty and T. J. Meyer), Elsevier, Dordrecht, 2004, chap. 16.
- 14 Special issues on DSSC: *Coord. Chem. Rev.*, 2004, 248, pp. 1161–1530.
- 15 M. K. Nazeeruddin, A. Kay, I. Rodicio, R. Humphry-Baker, E. Mueller, P. Liska, N. Vlachopoulos and M. Grätzel, *J. Am. Chem. Soc.*, 1993, **115**, 6382–6390.
- 16 (a) M. K. Nazeeruddin, F. De Angelis, S. Fantacci, A. Selloni, G. Viscardi, P. Liska, S. Ito, B. Takeru and M. Grätzel, *J. Am. Chem. Soc.*, 2005, **127**, 16835–16847; (b) M. K. Nazeeruddin, R. Splivallo, P. Liska, P. Comte and M. Grätzel, *Chem. Commun.*, 2003, 1456–1457.
- 17 (a) P. Wang, S. M. Zakeeruddin, I. Exnar and M. Grätzel, *Chem. Commun.*, 2002, 2972–2973; (b) P. Wang, S. M. Zakeeruddin, J. E. Moser, M. K. Nazeeruddin, T. Sekiguchi and M. Grätzel, *Nat. Mater.*, 2003, **2**, 402–407; (c) P. Wang, B. Wenger, R. Humphry-Baker, J. E. Moser, J. Teuscher, W. Kantelehner, J. Mezger, E. V. Stoyanov, S. M. Zakeeruddin and M. Grätzel, *J. Am. Chem. Soc.*, 2005, **127**, 6850–6856.
- 18 (a) M. K. Nazeeruddin, P. Pechy, T. Renouard, S. M. Zakeeruddin, R. Humphry-Baker, P. Comte, P. Liska, L. Cevey, E. Costa, V. Shklover, L. Spiccia, G. B. Deacon, C. A. Bignozzi and M. Grätzel, *J. Am. Chem. Soc.*, 2001, **123**, 1613–1624; (b) Y. Chiba, A. Islam, Y. Watanabe, R. Komiya, N. Koide and L. Han, *Jpn. J. Appl. Phys.*, 2006, **45**, L638–L640; (c) M. K. Nazeeruddin, P. Pechy and M. Grätzel, *Chem. Commun.*, 1997, 1705–1706.
- 19 M. Yanagida, L. P. Singh, K. Sayama, K. Hara, R. Katoh, A. Islam, H. Sugihara, H. Arakawa, M. K. Nazeeruddin and M. Grätzel, *J. Chem. Soc., Dalton Trans.*, 2000, 2817–2822.
- 20 (a) C. Y. Chen, S. J. Wu, C. G. Wu, J. G. Chen and K. C. Ho, *Angew. Chem., Int. Ed.*, 2006, **45**, 5822–5825; (b) K.-J. Jiang, N. Masaki, J. Xia, S. Noda and S. Yanagida, *Chem. Commun.*, 2006, 2460–2462; (c) A. Abbotto, C. Barolo, L. Bellotto, F. De Angelis, M. Grätzel, N. Manfredi, C. Marinzi, S. Fantacci, J.-H. Yum and M. K. Nazeeruddin, *Chem. Commun.*, 2008, 5318–5320; (d) D. Shi, N. Pootrakulchote, R. Li, J. Gui, Y. Wang, S. M. Zakeeruddin, M. Grätzel and P. Wang, *J. Phys. Chem. C*, 2008, **112**, 17046–17050; (e) C.-Y. Chen, S.-J. Wu, J.-Y. Li, C.-G. Wu, J.-G. Chen and K.-C. Ho, *Adv. Mater.*, 2007, **19**, 3888–3891; (f) J.-F. Yin, D. Bhattacharya, Y.-C. Hsu, C.-C. Tsai, K.-L. Lu, H.-C. Lin, J.-G. Chen and K.-C. Ho, *J. Mater. Chem.*, 2009, **19**, 7036–7042.
- 21 F. Gao, Y. Wang, D. Shi, J. Zhang, M. Wang, X. Jing, R. Humphry-Baker, P. Wang, S. M. Zakeeruddin and M. Grätzel, *J. Am. Chem. Soc.*, 2008, **130**, 10720–10728.
- 22 C. Y. Chen, J. G. Chen, S. J. Wu, J. Y. Li, C. G. Wu and K. C. Ho, *Angew. Chem., Int. Ed.*, 2008, **47**, 7342–7345.
- 23 F. Gao, Y. Wang, J. Zhang, D. Shi, M. Wang, R. Humphry-Baker, P. Wang, S. M. Zakeeruddin and M. Grätzel, *Chem. Commun.*, 2008, 2635–2637.
- 24 Y. Hou, P. Xie, B. Zhang, Y. Cao, X. Xiao and W. Wang, *Inorg. Chem.*, 1999, **38**, 6320–6322.
- 25 F. M. Romero and R. Ziessel, *Tetrahedron Lett.*, 1995, **36**, 6471–6474.
- 26 J. I. Bruce, J.-C. Chambron, P. Kolle and J.-P. Sauvage, *J. Chem. Soc., Perkin Trans. 1*, 2002, 1226–1231.
- 27 G. Maerker and F. H. Case, *J. Am. Chem. Soc.*, 1958, **80**, 2745–2748.
- 28 D. Wenkert and R. B. Woodward, *J. Org. Chem.*, 1983, **48**, 283–289.

- 29 S. A. Haque, S. Handa, K. Peter, E. Palomares, M. Thelakkat and J. R. Durrant, *Angew. Chem., Int. Ed.*, 2005, **44**, 5740–5744.
- 30 K. Nonomura, Y. Xu, T. Marinado, D. P. Hagberg, R. Zhang, G. Boschloo, L. Sun and A. Hagfeldt, *Int. J. Photoenergy*, 2009, Article ID 471828(1–9).
- 31 J.-J. Kim, H. Choi, C. Kim, M.-S. Kang, H. S. Kang and J. Ko, *Chem. Mater.*, 2009, **21**, 5719–5726.
- 32 C. S. Karthikeyan, H. Wietasch and M. Thelakkat, *Adv. Mater.*, 2007, **19**, 1091–1095.
- 33 K. Willinger, K. Fischer, R. Kisselev and M. Thelakkat, *J. Mater. Chem.*, 2009, **19**, 5364–5376.
- 34 F. Lenzmann, J. Krueger, S. Burnside, K. Brooks, M. Grätzel, D. Gal, S. Rühle and D. Cahen, *J. Phys. Chem. B*, 2001, **105**, 6347–6352.
- 35 C.-Y. Chen, H.-C. Lu, C.-G. Wu, J.-G. Chen and K.-C. Ho, *Adv. Funct. Mater.*, 2007, **17**, 29–36.
- 36 (a) S. A. Haque, E. Palomares, B. M. Cho, A. N. M. Green, N. Hirata, D. R. Klug and J. R. Durrant, *J. Am. Chem. Soc.*, 2005, **127**, 3456–3462; (b) Z. S. Wang, H. Kawauchi, T. Kashima and H. Arakawa, *Coord. Chem. Rev.*, 2004, **248**, 1381–1389.
- 37 D. Miyoshi, H. Karimata, Z. M. Wang, K. Koumoto and N. Sugimoto, *J. Am. Chem. Soc.*, 2007, **129**, 5919–5925.
- 38 C.-G. Wu, Y.-C. Lin, C.-E. Wu and P.-H. Huang, *Polymer*, 2005, **46**, 3748–3757.
- 39 R. Pudzich and J. Salbeck, *Synth. Met.*, 2003, **138**, 21–31.
- 40 W. Li, C. Du, F. Li, Y. Zhou, M. Fahlman, Z. Bo and F. Zhang, *Chem. Mater.*, 2009, **21**, 5327–5334.
- 41 M. J. Frisch, G. W. Trucks, H. B. Schlegel, G. E. Scuseria, M. A. Robb, J. R. Cheeseman, J. A. Montgomery, Jr., T. Vreven, K. N. Kudin, J. C. Burant, J. M. Millam, S. S. Iyengar, J. Tomasi, V. Barone, B. Mennucci, M. Cossi, G. Scalmani, N. Rega, G. A. Petersson, H. Nakatsuji, M. Hada, M. Ehara, K. Toyota, R. Fukuda, J. Hasegawa, M. Ishida, T. Nakajima, Y. Honda, O. Kitao, H. Nakai, M. Klene, X. Li, J. E. Knox, H. P. Hratchian, J. B. Cross, V. Bakken, C. Adamo, J. Jaramillo, R. Gomperts, R. E. Stratmann, O. Yazyev, A. J. Austin, R. Cammi, C. Pomelli, J. W. Ochterski, P. Y. Ayala, K. Morokuma, G. A. Voth, P. Salvador, J. J. Dannenberg, V. G. Zakrzewski, S. Dapprich, A. D. Daniels, M. C. Strain, O. Farkas, D. K. Malick, A. D. Rabuck, K. Raghavachari, J. B. Foresman, J. V. Ortiz, Q. Cui, A. G. Baboul, S. Clifford, J. Cioslowski, B. B. Stefanov, G. Liu, A. Liashenko, P. Piskorz, I. Komaromi, R. L. Martin, D. J. Fox, T. Keith, M. A. Al-Laham, C. Y. Peng, A. Nanayakkara, M. Challacombe, P. M. W. Gill, B. Johnson, W. Chen, M. W. Wong, C. Gonzalez and J. A. Pople, *Gaussian 03, Revision B.*, Gaussian, Inc., Pittsburgh, PA, 2003.
- 42 (a) A. D. Becke, *Phys. Rev. A: At., Mol., Opt. Phys.*, 1988, **38**, 3098–3100; (b) A. D. Becke, *J. Chem. Phys.*, 1992, **96**, 2155–2160; (c) C. Lee, W. Yang and R. Parr, *Phys. Rev. B: Condens. Matter*, 1988, **37**, 785–789.
- 43 *SAINT+*, ver. 6.02a, Bruker Analytical X-ray System, Inc., Madison, WI, 1998.
- 44 G. M. Sheldrick, *SADABS*, Empirical Absorption Correction Program, University of Göttingen, Germany, 1997.
- 45 G. M. Sheldrick, *SHELXTL™*, Reference Manual, ver. 5.1, Madison, WI, 1997.